Kidney360

Interferon Regulatory Factor-5 in Resident Macrophage Promotes Polycystic Kidney Disease

Kurt A. Zimmerman,[1] Jifeng Huang,[2] Lan He,[2] Dustin Z. Revell,[1] Zhang Li,[1] Jung-Shan Hsu,[2] Wayne R. Fitzgibbon,[3] E. Starr Hazard,[4] Gary Hardiman,[5] Michal Mrug,[2,6] P. Darwin Bell,[2] Bradley K. Yoder,[1] and Takamitsu Saigusa[2]

Abstract

Background Autosomal dominant polycystic kidney disease is caused by genetic mutations in *PKD1* or *PKD2*. Macrophages and their associated inflammatory cytokines promote cyst progression; however, transcription factors within macrophages that control cytokine production and cystic disease are unknown.

Methods In these studies, we used conditional *Pkd1* mice to test the hypothesis that macrophage-localized interferon regulatory factor-5 (IRF5), a transcription factor associated with production of cyst-promoting cytokines (TNFα, IL-6), is required for accelerated cyst progression in a unilateral nephrectomy (1K) model. Analyses of quantitative real-time PCR (qRT-PCR) and flow-cytometry data 3 weeks post nephrectomy, a time point before the onset of severe cystogenesis, indicate an accumulation of inflammatory infiltrating and resident macrophages in 1K *Pkd1* mice compared with controls. qRT-PCR data from FACS cells at this time demonstrate that macrophages from 1K *Pkd1* mice have increased expression of *Irf5* compared with controls. To determine the importance of macrophage-localized *Irf5* in cyst progression, we injected scrambled or IRF5 antisense oligonucleotide (ASO) in 1K *Pkd1* mice and analyzed the effect on macrophage numbers, cytokine production, and renal cystogenesis 6 weeks post nephrectomy.

Results Analyses of qRT-PCR and IRF5 ASO treatment significantly reduced macrophage numbers, *Irf5* expression in resident—but not infiltrating—macrophages, and the severity of cystic disease. In addition, IRF5 ASO treatment in 1K *Pkd1* mice reduced *Il6* expression in resident macrophages, which was correlated with reduced STAT3 phosphorylation and downstream p-STAT3 target gene expression.

Conclusions These data suggest that *Irf5* promotes inflammatory cytokine production in resident macrophages resulting in accelerated cystogenesis.

KIDNEY360 1: 179–190, 2020. doi: https://doi.org/10.34067/KID.0001052019

Introduction

Autosomal dominant polycystic kidney disease (ADPKD) is caused by mutations in *polycystic kidney disease 1 (PKD1)* or *PKD2*, which encodes for protein polycystin 1 and polycystin 2, respectively (1). Disease progression is highly variable, even among family members that share identical *PKD1* mutations (2). A possible mechanism explaining the variability in phenotypic progression is the presence of "modifying factors" that can accelerate cyst growth in the presence of *PKD* mutations (3–6). Renal injury is one example of a modifier that can accelerate cystogenesis (3,6–11). We have shown that unilateral nephrectomy (UNx) in adult conditional *Pkd1* knockout mice leads to accelerated cyst growth (6,9). A hallmark of UNx is compensatory renal hypertrophy triggered by increased GFR and protein synthesis (12,13). Thus, we propose that the increased workload and exposure to hypertrophic factors (*i.e.*, amino acids (14)) in the remaining kidney promotes enhanced cystogenesis in mice lacking *Pkd1*. The mechanism connecting renal hypertrophy and accelerated cystogenesis is unknown.

Among a number of factors that are involved in the pathogenesis of PKD, recent evidence suggests that innate immunity, particularly macrophages, plays a significant role in cyst development (11,15–21). These studies demonstrated that there are an increased number of macrophages in cystic kidneys and that these macrophages drive proinflammatory cytokine–mediated tubular cell injury, proliferation, and cyst formation (15–19). Genetic deletion of *Ccl2* (*Mcp1*) significantly reduced the influx of macrophages to the kidney, lessened tubular cell injury, and reduced cyst growth (15,22). However, the importance of infiltrating macrophages may be model specific because genetic deletion of CCR2, the *Ccl2* ligand, did not affect cyst severity in the *cpk* mouse model (23). Of interest, our recent data also indicate that inhibition of resident

[1]Department of Cell, Developmental, and Integrative Biology, University of Alabama at Birmingham, Birmingham, Alabama; [2]Division of Nephrology, Department of Medicine, University of Alabama at Birmingham, Birmingham, Alabama; [3]Division of Nephrology, Department of Medicine, Medical University of South Carolina, Charleston, South Carolina; [4]Academic Affairs Faculty and Computational Biology Resource Center, Medical University of South Carolina, Charleston, South Carolina; [5]School of Biological Sciences, Institute for Global Food Security, Queens University Belfast, Belfast, United Kingdom; and [6]Birmingham Veterans Affairs Medical Center, Birmingham, Alabama

Correspondence: Dr. Takamitsu Saigusa, University of Alabama at Birmingham, LHRB621 1720 2nd Avenue South, Birmingham, AL 35294. Email: tsaigusa@uabmc.edu

macrophage proliferation and accumulation results in a significant reduction in cyst severity (11). Regardless of the source of macrophages, these cells are able to release inflammatory cytokines that promote cyst growth. However, intrinsic factors within macrophages that control production of inflammatory cytokines involved in cystic disease have not been identified.

IFN regulatory factor 5 (IRF5) is a transcription factor that has recently been identified as a mediator of proinflammatory cytokine production in macrophages. IRF5 is found in the cytoplasm of quiescent cells and upon stimulation becomes activated *via* post-translational modification. This results in nuclear translocation and binding to the promoter region of target genes, many of which are involved in proinflammatory responses (24). IRF5 is highly expressed in proinflammatory macrophages; promotes polarization of macrophages to an M1-like phenotype; and controls the production of inflammatory cytokines such as IL-6, TNF-α, and IL-12 (25,26). Although macrophage activation promotes cystogenesis, the role of IRF5 in this process is unknown.

Herein, we show that UNx in conditional *Pkd1* mice results in increased macrophage accumulation and production of inflammatory cytokines. The enhanced inflammatory profile observed in *Pkd1*-deficient mice after UNx was paralleled by increased whole-kidney *Irf5* expression. qRT-PCR of flow-sorted cells indicates that kidney macrophages were the main cell type responsible for the increased whole-kidney *Irf5* expression. Treatment of conditional *Pkd1* mice receiving UNx with an IRF5 antisense oligonucleotide (ASO) decreased *Irf5* expression specifically in resident macrophages and resulted in reduced *Il6* proinflammatory cytokine production and cystic kidney disease. Overall, our data show that (*1*) kidney resident macrophage activation and *Il6* cytokine production is driven by *Irf5*, (*2*) *Irf5* plays an essential role in acceleration of cyst growth after UNx, and (*3*) IRF5 in macrophages is a novel therapeutic target for slowing kidney cyst growth.

Materials and Methods

Mouse and Genotyping

All procedures were conducted under protocols approved by the Medical University of South Carolina and University of Alabama at Birmingham (UAB) Institutional Animal Care and Use Committee and in accordance with the National Institutes of Health (NIH) Eighth Guide for the Care and Use of Laboratory Animals. Development of *Pkd1* floxed allele mice has been previously reported (27). *Pkd1* conditional knockout mice were generated by crossbreeding $Pkd1^{f/f}$ female mice with $Pkd1^{f/f}$ male mice that express tamoxifen-inducible systemic cre (CAGG-creER) (28). Genotyping was performed by PCR using primer sequences as previously described (27).

UNx

Both female and male adult *Pkd1* conditional floxed mice with and without cre (4–6 weeks old) were administered tamoxifen (9 mg/40 g body wt; Sigma-Aldrich, St. Louis, MO) dissolved in corn oil *via* intraperitoneal injection every other day for a total of three doses. At 3 weeks after cre induction, mice underwent left UNx or sham surgery. All surgeries were performed under isoflurane anesthesia (5% induction, 1.5%–2% maintenance) with the mice placed on a heated platform. All mice received carprofen (5 mg/kg) pre- and postoperatively until the mice showed no signs of clinical distress. Briefly, after mice were anesthetized, the left kidney was excised *via* a left-of-center dorsal incision, the renal pedicle was tied with 5-0 ethilon loops, and the kidney excised. At 3 or 6 weeks after nephrectomy or sham surgery, mice were euthanized and the kidney was harvested for flow cytometry, histology, and qRT-PCR.

UNx mice were randomly assigned to IRF5 ASO or scrambled ASO groups (N=8–11, equal sex per group, from equally distributed littermates) for a treatment duration of 3 or 6 weeks, respectively. ASOs dissolved in PBS were administered weekly *via* subcutaneous injections at 40 mg/kg per week. At the end of each experiment, the kidney was harvested for analysis.

Immunofluorescence Microscopy

After fixation and overnight cryopreservation in 30% sucrose, 8-μm thick optimal cutting temperature compound–embedded kidney tissue was fixed with 4% paraformaldehyde (PFA) for 10 minutes, permeabilized with 0.2% Triton X-100 for 8 minutes, and incubated in blocking solution (PBS with 1% BSA, 0.3% Triton X-100, 2% [vol/vol] donkey serum, and 0.02% sodium azide) for 30 minutes at room temperature. Sections were incubated in primary antibody overnight at 4°C according to manufacturer's recommendation, washed with PBS, and incubated with the appropriate secondary antibodies in blocking solution for 1 hour at room temperature. Primary antibodies included a rat anti-mouse F4/80 (catalog number 14-4801; clone BM8; eBioscience) and a FITC-conjugated lotus tetragonolobus agglutinin (LTA) (catalog number FL-1321; Vector Laboratories) antibody. Secondary antibodies included the following: Alexa Fluor 647–conjugated donkey anti-rat (catalog number 712-606-153; Jackson ImmunoResearch). After addition of secondary antibody, nuclei were stained by Hoechst nuclear stain (Sigma-Aldrich) and samples mounted using IMMU-MOUNT (Thermo). All fluorescence images were captured on a Nikon TI2 Eclipse (Nikon Instruments) spinning disc confocal microscope equipped with a Yokogawa $\times$1 disc (Yokogawa) on an Orca Flash 4.0 sCMOS (Hamamatsu) using a 40$\times$ Plan Fluor 1.3NA (Nikon Instruments) objective. Confocal images were processed and analyzed in NIS Elements version 5.0 software.

To identify p-Stat3 signaling, we used a modified version of recently described protocol (29). Paraffin-embedded sections were rehydrated using a xylene and decreasing ethanol series, washed in Tris-buffered saline (TBS), and boiled in 10 mM sodium citrate buffer (pH 6) for 5 minutes in a 100°C water bath. The sections were cooled, washed twice in TBS/Tween 20, and blocked (1% BSA, 0.05% sodium azide in TBS/Tween 20) at 37°C for 30 minutes. Sections were incubated with the following antibodies diluted in blocking buffer overnight at 4°C: p-STAT3 (Tyr705) rabbit mAb (9145; Cell Signaling) and FITC-conjugated LTA. Sections were then incubated with fluorescence-labeled secondary antibodies diluted in blocking buffer at 37°C for 1 hour (Alexa Fluor 647 donkey anti-rabbit IgG [catalog number A21244; Life Technologies]). After washing, nuclei were

stained by Hoechst nuclear stain before postfixing with 4% PFA for 10 minutes, and samples mounted using IMMU-MOUNT. Samples were imaged as described above.

ASOs

ASOs were obtained from Ionis Pharmaceuticals (Carlsbad, CA). Gen 2.5 IRF5 ASO were 16-mer constrained ethyl gapmers with a chimeric 3-10-3s with constrained ethyl design (sequence: AACATTTATTAATCCA), locking the 2′ and 4′ positions together to constrain the ribose ring into a C_3-endoconformation. The scramble ASO had the same design but does not hybridize to any known target and was used to control for any ASO class effects that could influence cystogenesis and/or kidney function. The scramble ASO used in this study was identical to ASOs previously described and can successfully target the kidney (30).

Flow Cytometry

After transcardial perfusion of the mouse with PBS, the right kidney was removed and placed into RPMI 1640 on ice. The kidneys were minced and digested in 1 ml of RPMI 1640 containing 1 mg/ml collagenase type I (Sigma-Aldrich) and 100 U/ml DNase I (Sigma-Aldrich) for 30 minutes at 37°C with agitation. Kidney fragments were passed through a 70-μm mesh (Falcon; BD Biosciences) yielding single-cell suspensions. Cells were centrifuged at 1300 rpm (220 $\times$ *g*) for 5 minutes at 4°C, resuspended in red blood cell lysis buffer, and incubated at 37°C for 5 minutes. Cells were resuspended in 1 ml PBS with Fc-blocking solution (dilution 1:200) and incubated for 30 minutes on ice. A total of 2×10^6 cells were stained for 30 minutes at room temperature with antibodies including phycoerythrin rat anti-mouse CD45 (catalog number 12-0451, 30-F11; eBioscience), eFluor450 rat anti-mouse F4/80 (catalog number 48-4801, BM8; eBioscience), allophycocyanin rat anti-mouse CD11b (catalog number 17-0112, M1/70; eBioscience), allophycocyanin/Cy7 rat anti-mouse Gr-1 (catalog number 557661, RB6-8C5; BD Pharmingen), phycoerythrin/Cy7 rat anti-mouse CD11c (catalog number 25-0114, N418; eBioscience), and FITC rat anti-mouse Ly6c (catalog number 553104, AL-21; BD Pharmingen); washed; and resuspended in FACS staining buffer. Cells were fixed in 2% PFA for 30 minutes at room temperature, washed, and resuspended in PBS. Cells were analyzed on a BD LSRII flow cytometer. To adjust for day-to-day fluctuations in the flow cytometer and antibody staining, macrophage gates were set using noninjured controls run on each individual day. Data analysis was performed using FlowJo version 10 software.

For qRT-PCR on flow-sorted populations, single cells were stained with markers to detect infiltrating and resident macrophages as described above (CD11b and F4/80) as well as the proximal tubule epithelium (FITC-conjugated LTA) and collecting duct epithelium (dolichos biflorus agglutinin [DBA; RL-1032; Vector Laboratories]). After incubation with primary antibody, cells were washed and resuspended in PBS. Cells were sorted into individual Eppendorf tubes containing RNA lysis buffer (buffer RLT; Qiagen) using a BD FACSCaliber AriaII. RNA was isolated using a Qiagen RNeasy Mini Kit (catalog number 74104; Qiagen) and cDNA synthesized with a High Capacity cDNA Reverse Transcription Kit (catalog number 4368813; Applied Biosystems).

qRT-PCR

After perfusion of the mouse with PBS, the right kidney was removed and placed into RNAlater (AM7020; Invitrogen). Total RNA was extracted using the Qiagen RNeasy Mini Kit and cDNA was synthesized with High Capacity cDNA Reverse Transcription Kit. An amount of 50 ng cDNA per reaction was used for qRT-PCR with TaqMan Gene Expression Master Mix (catalog number 4369016; Applied Biosystems) and Taqman probes for *Irf5* (Mm00496477), *Il-1b* (Mm00434228), *Il-6* (Mm00446190), *Tnf-a* (Mm00443258), *Il12* (Mm00434169), *Cx3cl1* (Mm00436454), *Csf1* (Mm00432686), *Ccl2* (Mm00441242), *Ccnd1* (Mm00432359), *Socs3* (Mm00545913), *C-myc* (Mm01192721), and *Tgfb* (Mm01188201). qRT-PCR was conducted with CFX96 Touch Real-Time PCR Detection System (Bio-Rad). Levels of the target genes were normalized against the housekeeping genes (*Gapdh*) and interpreted using the comparative ΔΔCt method. Human kidney tissues were obtained from patients who underwent nephrectomy either from ESKD secondary to PKD or non-PKD–related ESKD and were evaluated for *IRF5* (Hs00158114) expression (average age 45 years, both male and female). Data were normalized to *GAPDH* (Hs99999905). Kidney tissue was collected and processed according to previous publications (31) within 4 hours of resection according to a protocol approved by the UAB Institutional Review Board.

Quantification of Cystic Severity

Sections (5 μm) were cut from paraffin-embedded right kidneys and stained with hematoxylin and eosin. Hematoxylin and eosin–stained sections were used to determine cyst index. At least eight to ten different nonoverlapping kidney cortical sections (10×) were randomly taken from each of 90°, 180°, and 270° from the hilum to avoid field selection variation from all kidneys. Using Image J, the diameters of the tubular lumen were measured and counted as dilated tubules/cyst for those >40 μm. Mean cystic area relative to total kidney section area are shown as a percentage. A technician blinded to the treatment modality performed the quantification/analysis.

Statistical Analysis

Results are shown as means±SEM. Statistical difference between group means was determined by *t* test or one-way ANOVA followed by the Tukey test for multiple comparisons. All statistical tests were conducted using Prism 6 (GraphPad, La Jolla, CA). $P<0.05$ denoted statistical significance.

Results

UNx Promotes Kidney Immune Cell Accumulation and Inflammation in *Pkd1* Mouse

To determine whether accelerated cyst growth triggered by UNx promotes an immune cell response, we performed flow-cytometry analysis on single-cells isolated from kidneys harvested from adult *Pkd1* conditional mice (Cagg-Cre^{ERT2} *Pkd1*$^{f/f}$) 3 weeks after UNx (1K) or sham surgery (2K), a time point before the onset of severe cystogenesis. The 1K kidney histology at this time point shows dilated tubules and mild cysts compared to 2K kidney (Figure 1A). The gating strategy used to identify infiltrating and tissue-

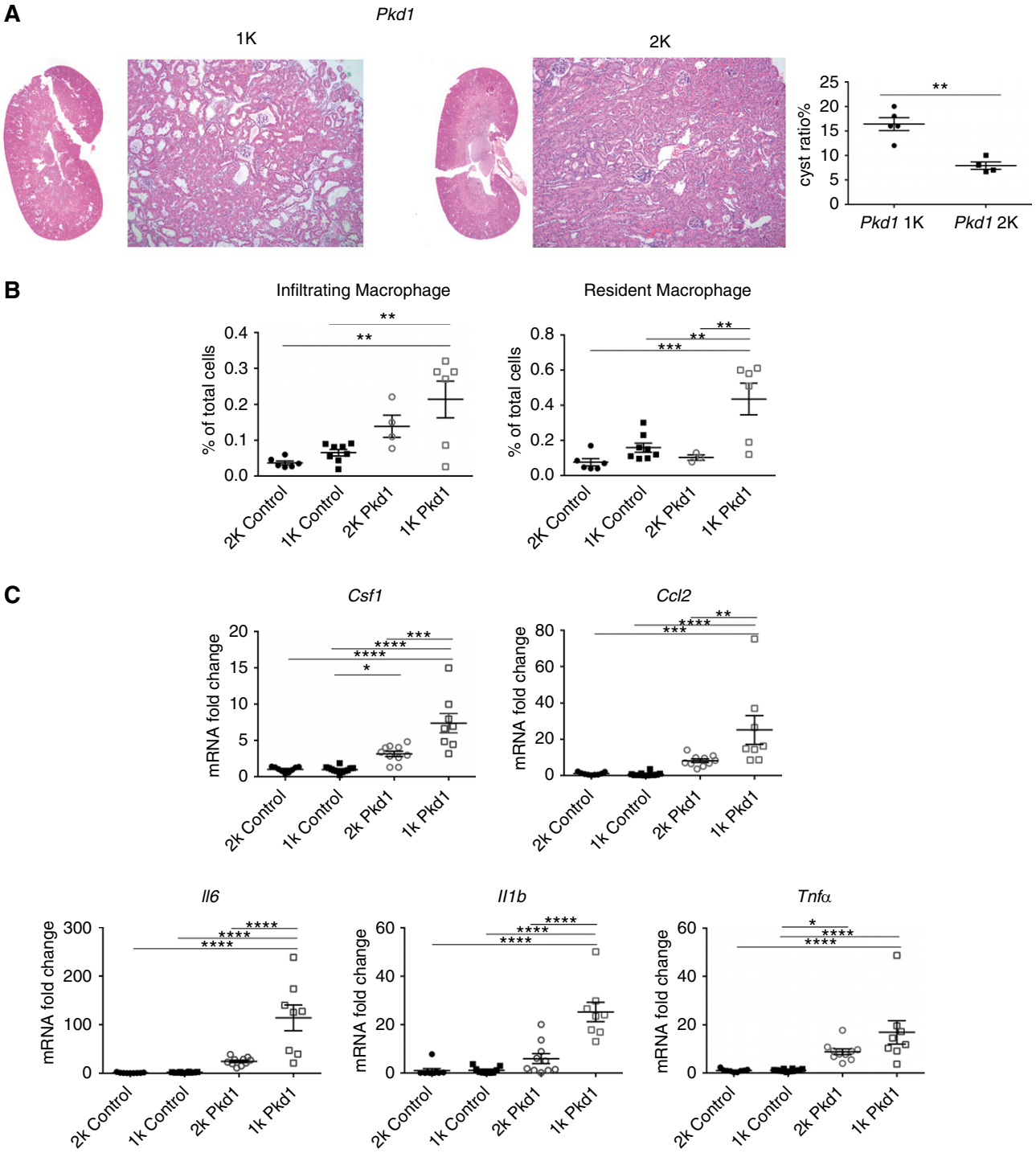

Figure 1. | 1K *Pkd1* mice have enhanced levels of macrophage chemoattractant cytokines and increased macrophage numbers compared with control kidneys. (A) Representative histology image of 1K and 2K kidneys taken from *Pkd1* mice 3 weeks after unilateral nephrectomy (UNx). There are dilated tubules and mild cyst formation in 1K *Pkd1* kidneys compared with 2K kidneys (magnification 20×). Quantification of cystic index is shown. (B) Number of kidney macrophages is shown as a percentage of total cells in 2K compared with 1K for both *Pkd1* and control mice. There was a significant increase in the number of kidney infiltrating and resident macrophages in 1K *Pkd1* kidneys compared with both 1K and 2K control kidneys. There was also an increased number of resident macrophages in 1K *Pkd1* kidneys compared with 2K *Pkd1* kidneys. (C) Kidney cytokine mRNA levels are shown as fold change compared with 2K control kidney. *Csf1*, *Ccl2*, *Il6*, *Il1b*, and *Tnfa* mRNA levels were significantly higher in 1K *Pkd1* mice compared with both 1K control and 2K control mice. *Csf1*, *Ccl2*, *Il1b*, and Il6 levels were higher in 1K *Pkd1* compared with 2K *Pkd1* mice. ****$P<0.0001$, ***$P<0.001$, **$P<0.01$, *$P<0.05$, *t* test or one-way ANOVA with multiple comparisons with Tukey test. 1K, 1 kidney; 2K, 2 kidney.

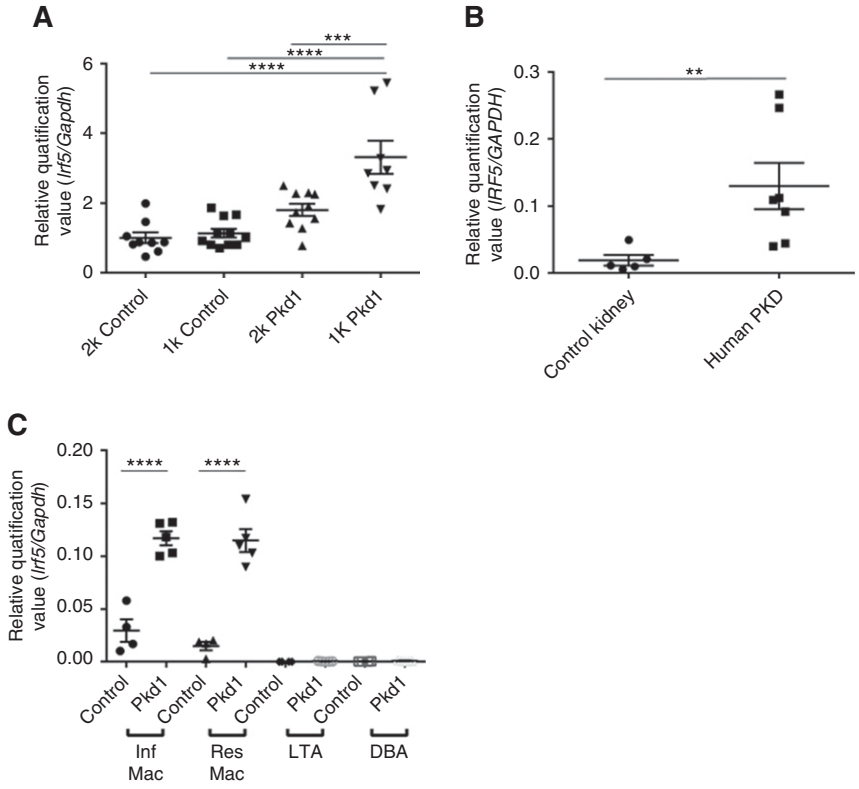

Figure 2. | *Irf5* expression is increased in kidneys isolated from *Pkd1* mice and patients with autosomal dominant polycystic kidney disease (ADPKD). (A) Quantitative real-time PCR (qRT-PCR) analysis of whole-kidney *Irf5* expression in control and *Pkd1* kidneys 3 weeks post-UNx or sham surgery. Our data indicate that 1K *Pkd1* kidneys had significantly increased levels of *Irf5* expression compared with control (both 1K and 2K, ****$P<0.0001$) and 2K *Pkd1* kidneys (***$P<0.001$, ****$P<0.0001$). (B) qRT-PCR analysis of whole-kidney *IRF5* expression in tissue harvested from patients with ADPKD and controls. There is increased kidney *IRF5* levels in patients with ADPKD compared with control patients (**$P<0.01$). (C) qRT-PCR analysis of *Irf5* expression in flow-sorted infiltrating macrophages, resident macrophages, lotus tetragonolobus agglutinin (LTA^+) proximal tubule epithelium, and dolichos biflorus agglutinin+ (DBA^+) collecting duct epithelium from wild-type and *Pkd1* mice kidneys (3 weeks post-UNx). Each dot represents an individual mouse kidney ($N=4–5$ mice per group). *Irf*5 was detected both in infiltrating and resident macrophage, but was not detected in proximal tubule (LTA^+) and collecting duct (DBA^+) epithelium in wild-type or 1K *Pkd1* mice. *Irf5* levels in infiltrating and resident macrophage from 1K *Pkd1* mice kidneys were significantly higher compared with wild-type kidneys (one-way ANOVA). GAPDH, glyceraldehyde 3-phosphate dehydrogenase; Inf Mac, infiltrating macrophages; PKD, polycystic kidney disease; Res Mac, resident macrophages.

resident macrophage populations in the kidney was based on differential expression of CD11b and F4/80, as previously published (Supplemental Figure 1) (11,32). Analysis of flow-cytometry data shows a significant increase in the number of infiltrating macrophages (as a percentage of total kidney cells) in 1K *Pkd1* mice compared with 1K and 2K cre-mice (Figure 1B). Further, our data indicate that the number of resident macrophages is significantly increased in 1K *Pkd1* mice compared with 2K *Pkd1* and control mice. These data indicate that UNx enhances the accumulation of macrophage populations in the kidney at early stages of cyst formation and suggests that these cells may promote cystic disease.

To gain insight into the inflammatory nature of kidney macrophages at this time, we performed qRT-PCR on whole-kidney tissue isolated 3 weeks post nephrectomy in control or *Pkd1* mice. qRT-PCR analysis revealed an increase in both macrophage chemoattractants and proinflammatory cytokines in 1K *Pkd1* kidneys compared with 2K *Pkd1* and control kidneys. This included macrophage chemokines and activators such as *Csf1* and *Ccl2* as well as the proinflammatory cytokines *Il6* and *Il1b* (Figure 1C). Despite the enhanced accumulation of infiltrating and resident macrophages in 1K *Pkd1* mice compared with 2K *Pkd1* mice at this time point, levels of *Tnfα* were not different between 1K and 2K *Pkd1* mice (Figure 1C). Flow-cytometry and qRT-PCR data did not reveal a difference in macrophage number or inflammatory gene expression between sexes within each group.

Loss of *Pkd1* Results in Increased Kidney *Irf5* Levels

Our data indicate that UNx in conditional *Pkd1* mice results in increased macrophage numbers, and a robust increase in proinflammatory cytokine production. However, factors within the macrophage that modulate the production of inflammatory cytokines in PKD have not been identified. IRF5 is a transcription factor that is highly expressed in macrophages during inflammation and promotes proinflammatory macrophage polarization

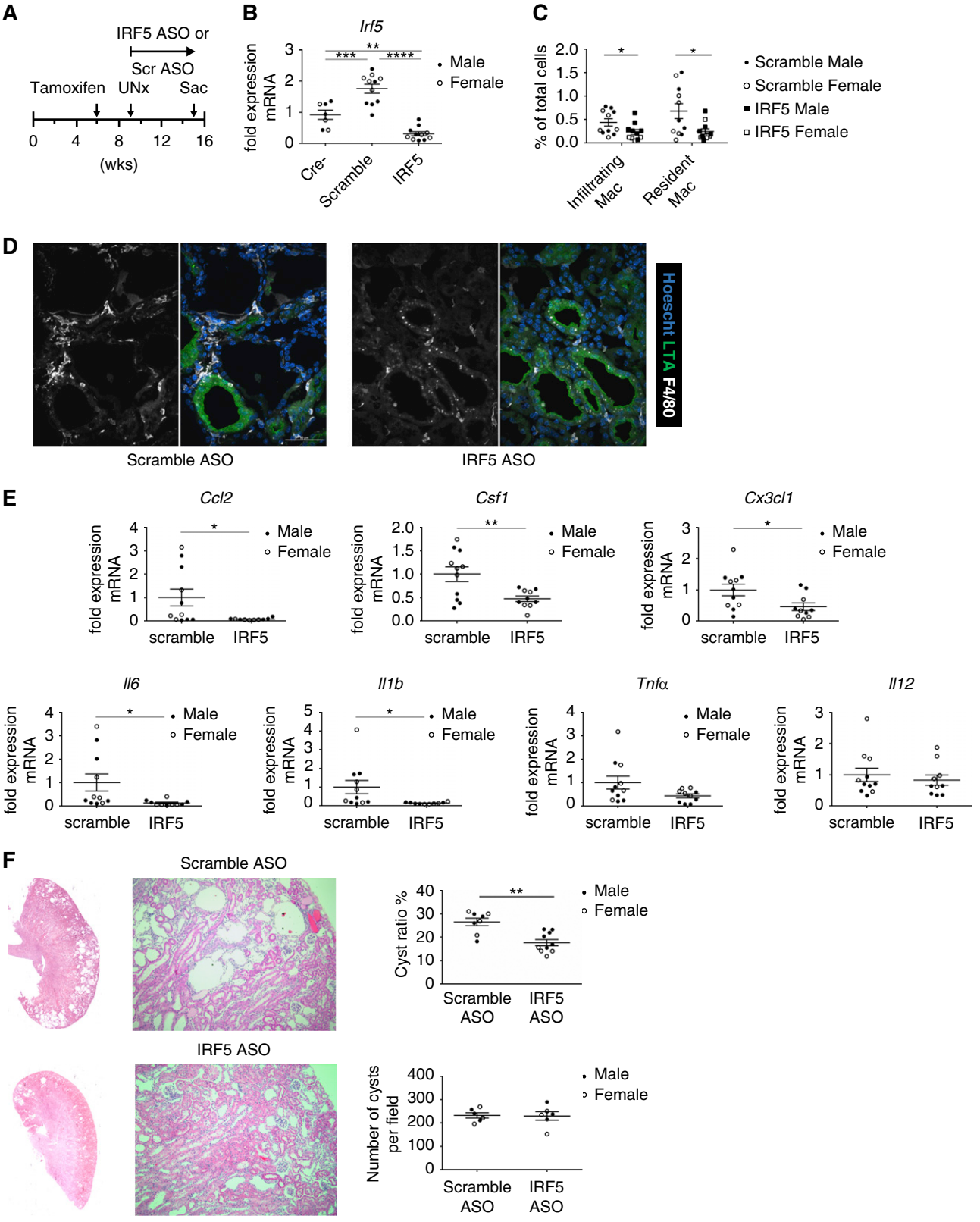

Figure 3. | Treatment of 1K *Pkd1* mice with IRF5 antisense oligonucleotide (ASO) significantly reduces macrophage accumulation, proinflammatory gene expression, and renal cystic disease. (A) Treatment protocol for mice receiving IRF5 or scrambled (Scr) ASO. (B) Whole-kidney *Irf5* mRNA levels shown as fold change compared with control cre- kidney. There was significant suppression of kidney *Irf5* mRNA levels in 1K *Pkd1* IRF5 ASO-treated mice compared with 1K *Pkd1* scramble ASO-treated and control (cre-) mice (one-way ANOVA). $^{**}P<0.001$, $^{***}P<0.001$, $^{****}P<0.0001$. (C) Number of kidney macrophages shown as percentage of total kidney cells in 1K *Pkd1* IRF5 ASO- compared with *Pkd1* Cont.

and cytokine production such as IL-6, TNFα, and IL-12 (25,26). Because both macrophage number and proinflammatory cytokines were increased in 1K *Pkd1* mice compared with controls, we hypothesized that IRF5 may be involved in the pathogenesis of accelerated cystogenesis in *Pkd1* mice receiving UNx.

To test this hypothesis, we first measured *Irf5* mRNA levels in whole-kidney tissue isolated from *Pkd1* and control mice 3 weeks post nephrectomy or sham surgery. As shown in Figure 2A, 1K *Pkd1* mice had significantly higher kidney *Irf5* mRNA levels compared with 2K *Pkd1* and control mice. Similarly, analysis of qRT-PCR data show increased kidney *IRF5* levels in human patients with ADPKD compared with controls (Figure 2B).

To determine the cell type responsible for the increased *Irf5* mRNA levels observed in 1K *Pkd1* kidneys 3 weeks post nephrectomy, we isolated macrophage and epithelial cell populations from the kidney of wild-type and 1K *Pkd1* mice *via* flow cytometry and performed qRT-PCR for *Irf5*. Our data indicate that expression of *Irf5* is significantly increased in infiltrating and resident macrophages from 1K *Pkd1* mice compared with control mice (Figure 2C). In contrast, *Irf5* is not detectable in LTA^+ proximal tubule cells or DBA^+ collecting duct cells (Figure 2C). These data suggest that macrophages are the major cell type responsible for the increased *Irf5* levels observed in 1K *Pkd1* mice.

Suppressing *Irf5* Attenuates Kidney Immune Cell Accumulation, Inflammatory Gene Expression, and Slows Cyst Growth

Because 1K *Pkd1* mice have increased macrophage accumulation, proinflammatory cytokine production, and *Irf5* expression compared with controls, we used an ASO that inhibits the synthesis of IRF5 in 1K *Pkd1* mice to test the importance of this transcription factor in cystic disease. Adult conditional *Pkd1* mice underwent UNx 3 weeks after tamoxifen injection, followed by weekly treatment with IRF5 ASO or scramble ASO for a total of 6 weeks after nephrectomy. The 6-week time point was used to assess the importance of *Irf5* in cystic growth. After 6 weeks, mice were euthanized and the number of kidney macrophages, level of proinflammatory cytokines, and severity of cystic disease were analyzed (Figure 3A). Our data indicate that IRF5 ASO treatment in 1K *Pkd1* mice significantly reduced whole-kidney *Irf5* expression compared with 1K *Pkd1* mice receiving scrambled ASO treatment (Figure 3B). Flow-cytometry analysis of macrophage populations reveals a significant decrease in the number of kidney infiltrating and resident macrophages in mice receiving the IRF5 ASO compared with scramble ASO-treated mice (Figure 3C). Confocal immunofluorescence microscopy data revealed a strong accumulation of $F4/80^+$ macrophages in cystic regions of scramble ASO-treated mice (Figure 3D). In contrast, analysis of confocal images from IRF5 ASO-treated mice shows reduced macrophage accumulation. Importantly, we did not detect any differences in the number of macrophages between sexes after IRF5 ASO treatment.

Next, we analyzed the effect of IRF5 ASO treatment on whole-kidney mRNA levels of macrophage chemoattractants and proinflammatory cytokines. Our data indicate a significant reduction in macrophage chemoattractant cytokines including *Ccl2*, *Csf1*, and *Cx3cl1* in 1K *Pkd1* mice treated with IRF5 ASO compared with 1K *Pkd1* mice treated with scrambled ASO (Figure 3E). Further, there is a significant decrease in expression levels of *Il6* and *Il1b* in IRF5 ASO-treated mice compared with scramble ASO-treated groups (Figure 3E). We did not observe a difference in levels of *Tnfa* and *Il12* mRNA between treatment groups.

Our data indicate that treatment of 1K *Pkd1* mice with IRF5 ASO significantly reduces macrophage number and whole-kidney proinflammatory gene expression. To determine the effect that IRF5 ASO treatment has on cystic progression, we performed histologic analysis of kidney sections 6 weeks post-UNx. Treatment of 1K *Pkd1* mice with IRF5 ASO compared with scramble ASO significantly suppressed cystic index but did not affect the number of cysts (Figure 3F). Collectively, these results indicate that IRF5 ASO treatment decreased kidney *Irf5* levels, decreased the number of infiltrating and resident macrophages, reduced whole-kidney inflammatory cytokines, and slowed cyst growth in rapidly progressive *Pkd1* conditional mice.

Suppression of *Irf5* Reduces Macrophage Proinflammatory Cytokine Production

Our data indicate that IRF5 is predominantly expressed in macrophages and that treatment of 1K *Pkd1* mice with IRF5 ASO significantly reduces whole-kidney proinflammatory gene expression and cystic index compared with the 1K *Pkd1* scramble ASO-treated group. Based on these data, we hypothesize that IRF5 ASO treatment reduces cystic index by reducing the ability of macrophages to produce cyst-promoting cytokines such as TNFα and IL-6 (26). Both of these cytokines, and their associated downstream signaling pathways including p-STAT3, are expressed in renal macrophages (33,34) and have been implicated in progression of cystic disease (35–38). To test this hypothesis, we flow sorted

Figure 3. | *Continued.* scrambled ASO-treated mice. There was a significant reduction in number of infiltrating macrophages and resident macrophages after 6 weeks of treatment with IRF5 ASO compared with scramble ASO treatment (*$P<0.05$). (D) Representative confocal images of 1K *Pkd1* IRF5 or scrambled ASO-treated mice stained with F4/80 (white), LTA (green), and Hoescht (dark blue). Our data indicate that $F4/80^+$ macrophages accumulate in cystic regions of 1K *Pkd1* ASO-treated mice. The number of these cells was reduced upon IRF5 ASO treatment. $N=3$ mice per group. (E) Kidney cytokine mRNA levels shown as fold change compared to with ASO-treated group. There were significant reductions in *Ccl2*, *Csf1*, *Cx3cl1*, *Il6*, and *Il1b* mRNA levels after 6 weeks of IRF5 ASO treatment. There were no differences in mRNA levels for *Tnfa* ($P=0.07$) and *Il12* ($P=0.53$) between IRF5 and scramble ASO treatment groups (*t* test). *$P<0.05$, **$P<0.01$. (F) Kidney histology from 1K *Pkd1* mice treated with IRF5 ASO or scramble ASO. Quantification of the cystic index (percentage cystic area/total kidney area) and cystic number is shown as mean±SEM in the associated graphs. **$P<0.05$; *t* test or one-way ANOVA with multiple comparisons with Tukey test; $N=8$–11 mice per group. Sac, euthanized.

macrophage (infiltrating and resident) and epithelial populations (LTA$^+$ proximal tubule, DBA$^+$ collecting duct) from the kidney of 1K *Pkd1* mice treated with IRF5 or scrambled ASO 6 weeks post nephrectomy and performed qRT-PCR for *Irf5*, *Il6*, and *Tnfa*. Our data indicate that mRNA levels of *Irf5* are significantly reduced in resident, but not in infiltrating, macrophages (Figure 4A). Further, *Il6* expression is significantly reduced in resident macrophages isolated from IRF5 ASO-treated mice compared with mice receiving scrambled ASO (Figure 4B). There was no difference in expression levels of *Tnfa* in macrophages upon IRF5 ASO treatment (Figure 4C). *Irf5*, *Il6*, and *Tnfa* mRNA were not detected in the LTA$^+$ proximal tubular epithelium or in the DBA$^+$ collecting duct epithelium. Collectively, these data indicate that IRF5 ASO treatment specifically targets resident macrophages and results in decreased *Irf5* and *Il6* production in these cells.

To test whether IRF5 ASO treatment specifically reduced proinflammatory cytokine production in macrophages, we analyzed gene expression of the anti-inflammatory cytokines *Il10* and *Tgfb1* in whole-kidney tissue from 1K *Pkd1* scramble- or IRF5-treated mice 6 weeks post nephrectomy. The mRNA level for *Tgfb1* was reduced in 1K *Pkd1* IRF5 ASO-treated mice compared with controls, whereas mRNA levels of *Il10* were not different between groups (Supplemental Figure 2A). To determine whether reduced *Tgfb1* was due to a direct reduction in macrophage gene expression or a secondary consequence of reduced cystic disease, we performed qRT-PCR for *Tgfb1* in sorted macrophage and epithelial cell populations. We found that IRF5 ASO treatment did not reduce mRNA expression of *Tgfb1* in macrophages compared with scramble ASO (Supplemental Figure 2B), indicating that the reduced *Tgfb1* levels observed in the IRF5 ASO-treated kidney was secondary to reduced cystic disease. Further, these data suggest that IRF5 ASO treatment specifically reduces proinflammatory *Il6* expression with no effect on expression of the anti-inflammatory cytokines *Tgfb1* and *Il10.*

Irf5 Suppression Reduces STAT3 Phosphorylation and Expression of p-STAT3 Target Genes in 1K *Pkd1* Mice

Because IRF5 ASO treatment reduced *Irf5* and *Il6* expression in kidney resident macrophages, we hypothesized that IL-6 accelerates cyst growth. IL-6 is a proinflammatory

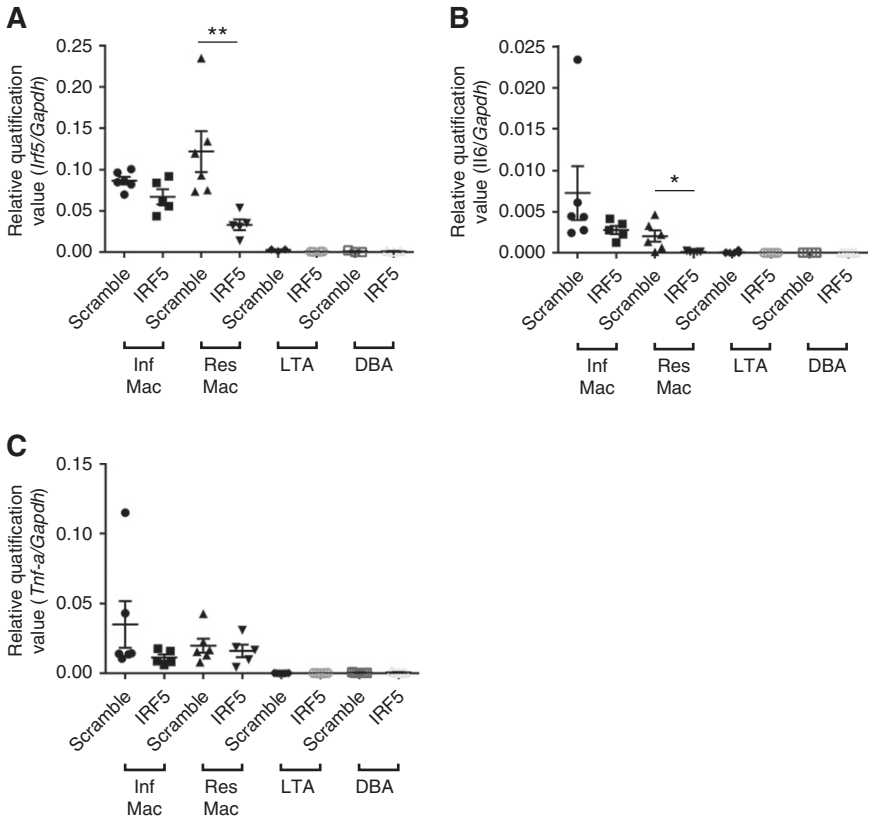

Figure 4. | **Treatment of 1K *Pkd1* mice with IRF5 ASO reduces *Irf5* and *Il6* expression in resident, but not infiltrating, macrophages.** (A) qRT-PCR analysis of *Irf5* expression in flow-sorted cells from 1K *Pkd1* mice treated with IRF5 or scrambled ASO for 6 weeks. mRNA levels for *Irf5* were significantly lower in IRF5 ASO-treated kidney resident macrophages compared with scramble ASO-treated resident macrophages (**$P<0.01$, two way ANOVA). There were no differences in level of *Irf5* in infiltrating macrophages upon IRF5 ASO treatment. *Irf5* was not detected in either epithelial population. (B) *Il6* mRNA levels are significantly lower in resident macrophages isolated from 1K *Pkd1* IRF5 ASO mice compared with 1K *Pkd1* scramble ASO-treated mice (*$P<0.05$, two way ANOVA). There were no differences in *Il6* expression in infiltrating macrophages, LTA$^+$ epithelium, or DBA$^+$ epithelium between IRF5 ASO- and scramble ASO-treated mice. Data are shown as the mean±SEM. (C) *Tnfa* mRNA expression was not different between treatment groups. Data are shown as the mean±SEM.

cytokine that signals through the JAK/STAT pathway resulting in STAT3 phosphorylation; nuclear translocation; and induction of p-STAT3 target genes including *Socs3*, *Ccnd1*, and *C-myc* (39,40). To determine the effect that IRF5 ASO treatment had on IL-6–dependent signaling in the epithelium, we analyzed confocal microscopy images that were obtained from kidney tissue that had been stained with a p-STAT3 antibody. Our data indicate that IRF5 ASO treatment of 1K *Pkd1* mice resulted in reduced nuclear p-STAT3 protein in the epithelia compared with 1K *Pkd1* mice receiving scrambled ASO (Figure 5A). These data are in agreement with previous reports indicating that reduction of p-STAT3 signaling is associated with improved renal cystic disease (38,39,41).

To confirm that IRF5 ASO treatment in 1K *Pkd1* mice resulted in a reduction of p-STAT3–dependent signaling, we analyzed expression of p-STAT3 target genes in whole-kidney tissue. We found that expression of *Socs3* and *C-myc* were both significantly reduced in 1K *Pkd1* mice receiving IRF5 ASO compared with 1K *Pkd1* mice receiving scrambled ASO (Figure 5B). There was no difference for *Ccnd1* between IRF5 ASO- and scramble ASO-treated kidney. Collectively, these data indicate that expression of p-STAT3 target genes is dampened after treatment with IRF5 ASO.

Discussion

This study revealed that (*1*) the number of kidney macrophages are increased in an accelerated PKD mouse model triggered by renal hypertrophic signaling; (*2*) there is increased kidney *Irf5* expression in patients with ADPKD and in our orthologous mouse model; (*3*) suppressing *Irf5* with an ASO reduces the number of kidney macrophages, inflammatory gene expression, and slows cyst growth; and (*4*) treatment of 1K *Pkd1* mice with IRF5 ASO resulted in reduced *Irf5* and *Il6* expression in resident macrophages and a correlative reduction in downstream p-STAT3 target gene activation compared with controls. The importance of macrophages during cyst progression in mouse models of cystic kidney disease has been reported (15–19). In these studies, we identify a transcription factor expressed by kidney resident macrophages, *Irf5*, that is responsible for *Il6* production and rapid cystic growth in adult *Pkd1* mice receiving UNx. These data suggest that targeting resident macrophages may be an effective treatment in PKD.

It is known that loss of renal mass (*i.e.*, removal of one kidney) decreases GFR. The decrease in GFR is followed by a period of hyperfiltration in the contralateral kidney resulting in recovered renal function (42). The initial decrease in GFR leads to an increased load of humoral factors to the contralateral kidney, which triggers compensatory renal

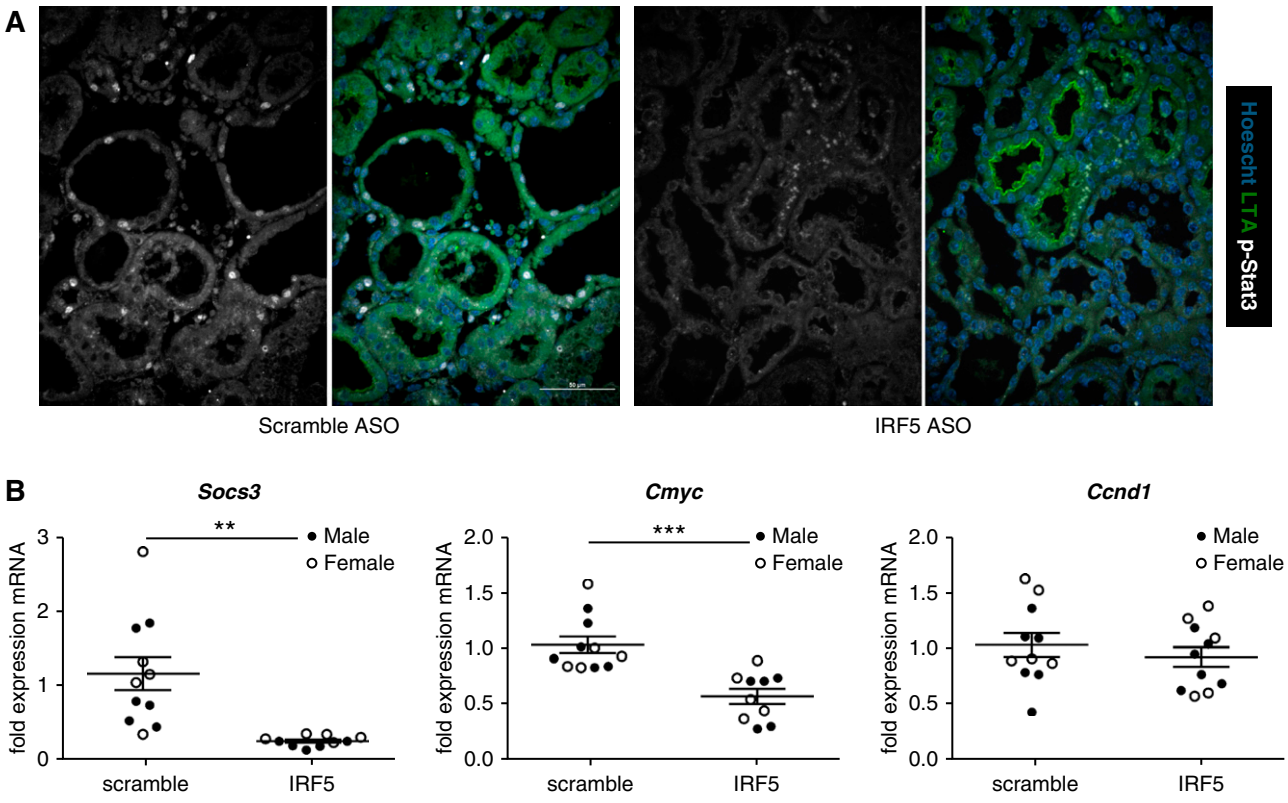

Figure 5. | 1K *Pkd1* IRF5 ASO-treated mice have reduced STAT3 phosphorylation and expression of p-STAT3 target genes compared with scrambled ASO-treated mice. (A) Representative confocal images depicting p-STAT3 (white) expression in kidney tissue harvested from 1K *Pkd1* mice treated with IRF5 or scrambled ASO. There is increased p-STAT3 staining in cystic tubules in scramble ASO- compared with IRF5 ASO-treated mouse kidneys (40× objective). (B) qRT-PCR of whole-kidney tissue isolated from 1K *Pkd1* mice that were treated with IRF5 or scramble ASO shown as fold difference. Expression of *Socs3* and *C-myc* were significantly reduced in the IRF5-treated group (**$P<0.01$, ***$P<0.001$, *t* test). There was no difference in kidney *Cyclin D1* levels in IRF5 ASO treatment compared with scramble treatment. Expression of *Socs3*, *C-myc*, and *Cyclin D1* (*Ccnd1*) are shown as the mean±SEM.

hypertrophy characterized by tubular hypertrophy and modest tubular dilation (12,14,43). Therefore, the increased humoral load and tubular hypertrophy observed in the contralateral kidney may serve as a form of injury that triggers accumulation of macrophages leading to accelerated cystogenesis. Because UNx in wild-type mice does not increase the number of macrophages (44), the accumulation of kidney macrophages upon UNx specifically occurs in the absence of *Pkd1*.

An interesting observation of these studies is data showing that treatment of 1K *Pkd1* mice with IRF5 ASO significantly reduced cystic index (*i.e.*, cyst size), but did not affect cyst number. These data suggest that the observed inflammatory macrophage phenotype does not affect cyst initiation, but is required for cyst progression. This also suggests that other resident-macrophage factors are likely important for cystic disease. These data have important implications for patients with cystic disease because slowing the rate of cyst growth may have significant clinical benefits. Further, our data indicate that IRF5 ASO treatment specifically reduced *Irf5* expression in resident, but not infiltrating, macrophages. This effect may be due to the reported ability of kidney resident macrophages to uptake factors in the blood (45), the continual replenishment of infiltrating macrophages from the bone marrow (causing the infiltrating macrophages to have normal *Irf5* expression), or some combination of both possibilities. This suggests that ASO treatment may be an effective means to decrease gene expression specifically in kidney resident macrophages. Future studies focused on these questions are warranted.

Although macrophages are known to promote cystogenesis, factors that control the activation and cytokine-producing ability of these cells in cystic kidney disease have not been identified. Here we report that expression of *Irf5*, a transcription factor that modulates proinflammatory cytokine production, is increased in macrophages isolated from 1K *Pkd1* mice compared with controls. Treatment of mice with IRF5 ASO significantly reduced macrophage number, *Irf5* expression in resident but not infiltrating macrophages, proinflammatory cytokine production, and cystic severity. Treatment of 1K *Pkd1* mice with IRF5 ASO also resulted in decreased resident macrophage–localized *Il6* expression

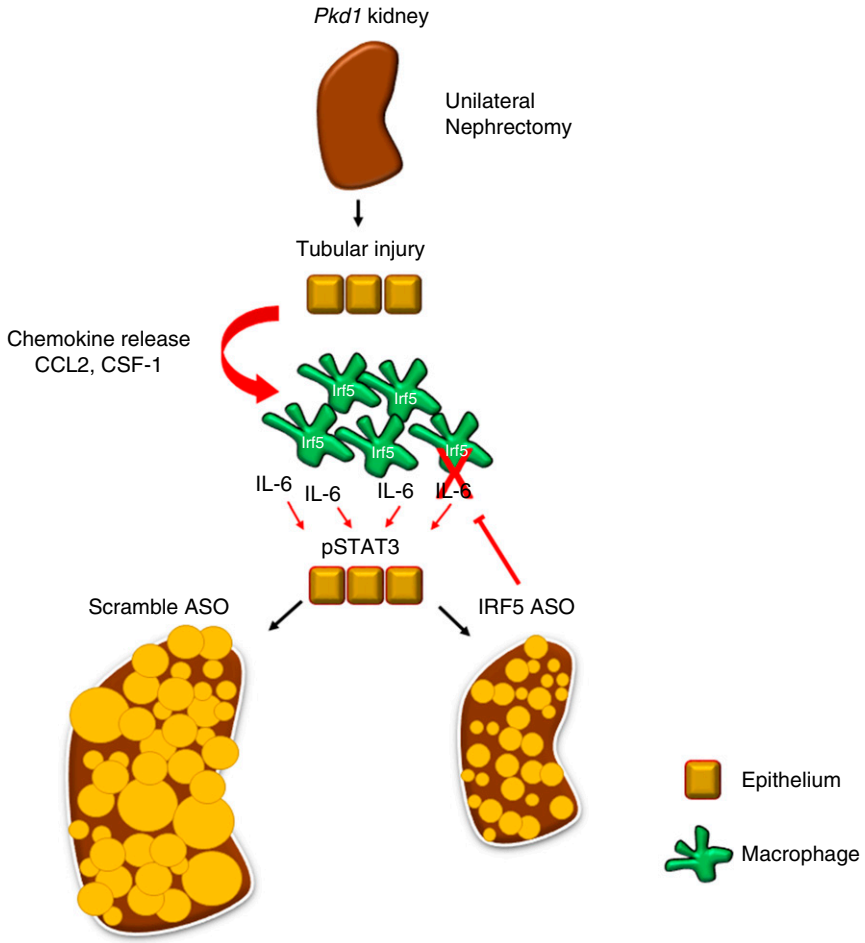

Figure 6. | **Proposed mechanism of IRF5-dependent cyst growth.** Unilateral nephrectomy causes renal hypertrophy–induced injury in *Pkd1* mice resulting in production of macrophage chemoattractant cytokines in kidney epithelium (*i.e.*, *Ccl2* and *Csf1*) and an accumulation of *Irf5*-expressing inflammatory macrophages. These *Irf5*-expressing macrophages release proinflammatory cytokines (IL-6) stimulating STAT3 phosphorylation and cyst growth in mice lacking *Pkd1*. Suppressing *Irf5* expression with ASO results in decreased cytokine production, reduced p-STAT3 in the epithelium, and slowed cyst growth.

and reduced STAT3 phosphorylation in the epithelium. Suppressing IRF5 synthesis decreased *Il6* but did not reduce *Tnfa* or the anti-inflammatory cytokine *Tgfb1* in macrophages, indicating that IRF5 ASO does not inhibit production of all cytokines. Although studies have shown that IRF5 promotes the release of IL-6, TNFα, and IL-12 (25,26), IRF5 ASO treatment did not affect the levels of TNFα and IL-12 in 1K *Pkd1* mice. These data suggest that the *Irf5*-expressing inflammatory macrophages stimulate *Pkd1*-deficient tubular epithelium by secreting IL-6 to drive p-STAT3–dependent cyst progression (Figure 6). With the recent discovery of a candidate resident macrophage population in humans (46), our data indicate that using ASOs may be an effective means to reduce cytokine production in these cells, reduce kidney inflammation, and slow cystic growth in human patients.

Acknowledgments

We thank Ionis Pharmaceutical for providing ASOs for IRF5 and scramble treatment.

Author Contributions

T. Saigusa and K. Zimmerman conceptualized the study, were responsible for visualization, wrote the original draft, and reviewed and edited the manuscript; G. Hardiman, E. Hazard, J. Huang, D. Revell, T. Saigusa, B. Yoder, and K. Zimmerman were responsible for data curation; G. Hardiman, E. Hazard, J. Huang, T. Saigusa, and K. Zimmerman were responsible for formal analysis; T. Saigusa, B. Yoder, and K. Zimmerman were responsible for funding acquisition; W. Fitzgibbon, G. Hardiman, E. Hazard, L. He, J. Hsu, J. Huang, Z. Li, M. Mrug, D. Revell, T. Saigusa, B. Yoder, and K. Zimmerman were responsible for investigation; E. Hazard, L. He, J. Huang, T. Saigusa, and K. Zimmerman were responsible for methodology; G. Hardiman, E. Hazard, J. Huang, D. Revell, T. Saigusa, and K. Zimmerman were responsible for validation; P. Bell, T. Saigusa, and B. Yoder were responsible for supervision; M. Mrug was responsible for resources; K. Zimmerman was responsible for project administration.

Disclosures

M. Mrug has received research/clinical trial support from and has consulted for Otsuka and Sanofi-Genzyme. The remaining authors have nothing to disclose.

Funding

G. Hardiman acknowledges support from NIH grant U01-DA045300. M. Mrug is supported by NIH National Institute of Diabetes and Digestive and Kidney Diseases (NIDDK) grant DK097423 and Office of Research and Development, Medical Research Service, US Department of Veterans Affairs grant 1I01-BX002298. M. Mrug and B. Yoder are supported by School of Medicine, UAB grant AMC21. T. Saigusa is supported by PKD Foundation grant 232G19a and NIH NIDDK grants K08 DK106465 and R03 DK119717. B. Yoder is supported by PKD Foundation grant 214g16a and NIH NIDDK grant R01 DK115752. K. Zimmerman is supported by NIH NIDDK T32 Basic Immunology and Immunologic Disease training grant 2T32-AI007051-38, the Baltimore PKD Center Pilot and Feasibility grant 2P30-DK090868, and UAB Hepatorenal Fibrocystic Disease Core Center Pilot and Feasibility grant 5P30-DK074038. The following NIH-funded cores provided services for this project: UAB Hepatorenal Fibrocystic Disease Core Center grant P30-DK074038, UAB-University of California, San Diego O'Brien Center for AKI Research grant P30-DK079337, and the UAB Comprehensive Flow Cytometry Core grants P30-AR048311 and P30-AI27667.

Supplemental Material

This article contains the following supplemental material online at http://kidney360.asnjournals.org/lookup/suppl/doi:10.34067/KID.0001052019/-/DCSupplemental.

Supplemental Figure 1. Gating strategy used to identify renal infiltrating and tissue resident macrophages.

Supplemental Figure 2. IRF5 ASO treatment does not reduce *Tgfb1* gene expression in sorted macrophages from 1K *Pkd1* mice.

References

1. Harris PC, Torres VE: Polycystic kidney disease. *Annu Rev Med* 60: 321–337, 2009
2. Rossetti S, Kubly VJ, Consugar MB, Hopp K, Roy S, Horsley SW, Chauveau D, Rees L, Barratt TM, van't Hoff WG, Niaudet P, Torres VE, Harris PC, Harris PC: Incompletely penetrant PKD1 alleles suggest a role for gene dosage in cyst initiation in polycystic kidney disease [published correction appears in *Kidney Int* 75: 1359, 2009]. *Kidney Int* 75: 848–855, 2009
3. Takakura A, Contrino L, Zhou X, Bonventre JV, Sun Y, Humphreys BD, Zhou J: Renal injury is a third hit promoting rapid development of adult polycystic kidney disease. *Hum Mol Genet* 18: 2523–2531, 2009
4. Patel V, Li L, Cobo-Stark P, Shao X, Somlo S, Lin F, Igarashi P: Acute kidney injury and aberrant planar cell polarity induce cyst formation in mice lacking renal cilia. *Hum Mol Genet* 17: 1578–1590, 2008
5. Happé H, Leonhard WN, van der Wal A, van de Water B, Lantinga-van Leeuwen IS, Breuning MH, de Heer E, Peters DJ: Toxic tubular injury in kidneys from Pkd1-deletion mice accelerates cystogenesis accompanied by dysregulated planar cell polarity and canonical Wnt signaling pathways. *Hum Mol Genet* 18: 2532–2542, 2009
6. Bell PD, Fitzgibbon W, Sas K, Stenbit AE, Amria M, Houston A, Reichert R, Gilley S, Siegal GP, Bissler J, Bilgen M, Chou PC, Guay-Woodford L, Yoder B, Haycraft CJ, Siroky B: Loss of primary cilia upregulates renal hypertrophic signaling and promotes cystogenesis. *J Am Soc Nephrol* 22: 839–848, 2011
7. Piontek K, Menezes LF, Garcia-Gonzalez MA, Huso DL, Germino GG: A critical developmental switch defines the kinetics of kidney cyst formation after loss of Pkd1. *Nat Med* 13: 1490–1495, 2007
8. Sharma N, Malarkey EB, Berbari NF, O'Connor AK, Vanden Heuvel GB, Mrug M, Yoder BK: Proximal tubule proliferation is insufficient to induce rapid cyst formation after cilia disruption. *J Am Soc Nephrol* 24: 456–464, 2013
9. Fitzgibbon WR, Dang Y, Bunni MA, Baicu CF, Zile MR, Mullick AE, Saigusa T: Attenuation of accelerated renal cystogenesis in Pkd1 mice by renin-angiotensin system blockade. *Am J Physiol Renal Physiol* 314: F210–F218, 2018
10. Sas KM, Yin H, Fitzgibbon WR, Baicu CF, Zile MR, Steele SL, Amria M, Saigusa T, Funk J, Bunni MA, Siegal GP, Siroky BJ, Bissler JJ, Bell PD: Hyperglycemia in the absence of cilia accelerates cystogenesis and induces renal damage. *Am J Physiol Renal Physiol* 309: F79–F87, 2015
11. Zimmerman KA, Song CJ, Li Z, Lever JM, Crossman DK, Rains A, Aloria EJ, Gonzalez NM, Bassler JR, Zhou J, Crowley MR, Revell DZ, Yan Z, Shan D, Benveniste EN, George JF, Mrug M, Yoder BK: Tissue-resident macrophages promote renal cystic disease. *J Am Soc Nephrol* 30: 1841–1856, 2019
12. Malt RA: Humoral factors in regulation of compensatory renal hypertrophy. *Kidney Int* 23: 611–615, 1983
13. Dicker SE, Shirley DG: Mechanism of compensatory renal hypertrophy. *J Physiol* 219: 507–523, 1971
14. Chen JK, Nagai K, Chen J, Plieth D, Hino M, Xu J, Sha F, Ikizler TA, Quarles CC, Threadgill DW, Neilson EG, Harris RC: Phosphatidylinositol 3-kinase signaling determines kidney size. *J Clin Invest* 125: 2429–2444, 2015

15. Cassini MF, Kakade VR, Kurtz E, Sulkowski P, Glazer P, Torres R, Somlo S, Cantley LG: Mcp1 promotes macrophage-dependent cyst expansion in autosomal dominant polycystic kidney disease. *J Am Soc Nephrol* 29: 2471–2481, 2018
16. Karihaloo A, Koraishy F, Huen SC, Lee Y, Merrick D, Caplan MJ, Somlo S, Cantley LG: Macrophages promote cyst growth in polycystic kidney disease. *J Am Soc Nephrol* 22: 1809–1814, 2011
17. Swenson-Fields KI, Vivian CJ, Salah SM, Peda JD, Davis BM, van Rooijen N, Wallace DP, Fields TA: Macrophages promote polycystic kidney disease progression. *Kidney Int* 83: 855–864, 2013
18. Chen L, Zhou X, Fan LX, Yao Y, Swenson-Fields KI, Gadjeva M, Wallace DP, Peters DJ, Yu A, Grantham JJ, Li X: Macrophage migration inhibitory factor promotes cyst growth in polycystic kidney disease. *J Clin Invest* 125: 2399–2412, 2015
19. Mrug M, Zhou J, Woo Y, Cui X, Szalai AJ, Novak J, Churchill GA, Guay-Woodford LM: Overexpression of innate immune response genes in a model of recessive polycystic kidney disease. *Kidney Int* 73: 63–76, 2008
20. Zimmerman KA, Song CJ, Gonzalez-Mize N, Li Z, Yoder BK: Primary cilia disruption differentially affects the infiltrating and resident macrophage compartment in the liver. *Am J Physiol Gastrointest Liver Physiol* 314: G677–G689, 2018
21. Song CJ, Zimmerman KA, Henke SJ, Yoder BK: Inflammation and fibrosis in polycystic kidney disease. *Results Probl Cell Differ* 60: 323–344, 2017
22. Viau A, Bienaimé F, Lukas K, Todkar AP, Knoll M, Yakulov TA, Hofherr A, Kretz O, Helmstädter M, Reichardt W, Braeg S, Aschman T, Merkle A, Pfeifer D, Dumit VI, Gubler MC, Nitschke R, Huber TB, Terzi F, Dengjel J, Grahammer F, Köttgen M, Busch H, Boerries M, Walz G, Triantafyllopoulou A, Kuehn EW: Cilia-localized LKB1 regulates chemokine signaling, macrophage recruitment, and tissue homeostasis in the kidney. *EMBO J* 37: e98615, 2018
23. Salah SM, Meisenheimer JD, Rao R, Peda JD, Wallace DP, Foster D, Li X, Li X, Zhou X, Vallejo JA, Wacker MJ, Fields TA, Swenson-Fields KI: MCP-1 promotes detrimental cardiac physiology, pulmonary edema, and death in the *cpk* model of polycystic kidney disease. *Am J Physiol Renal Physiol* 317: F343–F360, 2019
24. Barnes BJ, Kellum MJ, Field AE, Pitha PM: Multiple regulatory domains of IRF-5 control activation, cellular localization, and induction of chemokines that mediate recruitment of T lymphocytes. *Mol Cell Biol* 22: 5721–5740, 2002
25. Takaoka A, Yanai H, Kondo S, Duncan G, Negishi H, Mizutani T, Kano S, Honda K, Ohba Y, Mak TW, Taniguchi T: Integral role of IRF-5 in the gene induction programme activated by Toll-like receptors. *Nature* 434: 243–249, 2005
26. Krausgruber T, Blazek K, Smallie T, Alzabin S, Lockstone H, Sahgal N, Hussell T, Feldmann M, Udalova IA: IRF5 promotes inflammatory macrophage polarization and TH1-TH17 responses. *Nat Immunol* 12: 231–238, 2011
27. Piontek KB, Huso DL, Grinberg A, Liu L, Bedja D, Zhao H, Gabrielson K, Qian F, Mei C, Westphal H, Germino GG: A functional floxed allele of Pkd1 that can be conditionally inactivated in vivo. *J Am Soc Nephrol* 15: 3035–3043, 2004
28. Hayashi S, McMahon AP: Efficient recombination in diverse tissues by a tamoxifen-inducible form of Cre: A tool for temporally regulated gene activation/inactivation in the mouse. *Dev Biol* 244: 305–318, 2002
29. Torres JA, Rezaei M, Broderick C, Lin L, Wang X, Hoppe B, Cowley BD Jr, Savica V, Torres VE, Khan S, Holmes RP, Mrug M, Weimbs T: Crystal deposition triggers tubule dilation that accelerates cystogenesis in polycystic kidney disease. *J Clin Invest* 130: 4506–4522, 2019
30. Saigusa T, Dang Y, Mullick AE, Yeh ST, Zile MR, Baicu CF, Bell PD: Suppressing angiotensinogen synthesis attenuates kidney cyst formation in a Pkd1 mouse model. *FASEB J* 30: 370–379, 2016
31. Zimmerman KA, Gonzalez NM, Chumley P, Chacana T, Harrington LE, Yoder BK, Mrug M: Urinary T cells correlate with rate of renal function loss in autosomal dominant polycystic kidney disease. *Physiol Rep* 7: e13951, 2019
32. Schulz C, Gomez Perdiguero E, Chorro L, Szabo-Rogers H, Cagnard N, Kierdorf K, Prinz M, Wu B, Jacobsen SE, Pollard JW, Frampton J, Liu KJ, Geissmann F: A lineage of myeloid cells independent of Myb and hematopoietic stem cells. *Science* 336: 86–90, 2012
33. Awad AS, You H, Gao T, Cooper TK, Nedospasov SA, Vacher J, Wilkinson PF, Farrell FX, Brian Reeves W: Macrophage-derived tumor necrosis factor-α mediates diabetic renal injury. *Kidney Int* 88: 722–733, 2015
34. O'Leary R, Penrose H, Miyata K, Satou R: Macrophage-derived IL-6 contributes to ANG II-mediated angiotensinogen stimulation in renal proximal tubular cells. *Am J Physiol Renal Physiol* 310: F1000–F1007, 2016
35. Jing Y, Wu M, Zhang D, Chen D, Yang M, Mei S, He L, Gu J, Qi N, Fu L, Li L, Mei C: Triptolide delays disease progression in an adult rat model of polycystic kidney disease through the JAK2-STAT3 pathway. *Am J Physiol Renal Physiol* 315: F479–F486, 2018
36. Talbot JJ, Song X, Wang X, Rinschen MM, Doerr N, LaRiviere WB, Schermer B, Pei YP, Torres VE, Weimbs T: The cleaved cytoplasmic tail of polycystin-1 regulates Src-dependent STAT3 activation. *J Am Soc Nephrol* 25: 1737–1748, 2014
37. Wu M, Gu J, Mei S, Xu D, Jing Y, Yao Q, Chen M, Yang M, Chen S, Yang B, Qi N, Hu H, Wüthrich RP, Mei C: Resveratrol delays polycystic kidney disease progression through attenuation of nuclear factor κB-induced inflammation. *Nephrol Dial Transplant* 31: 1826–1834, 2016
38. Leonhard WN, van der Wal A, Novalic Z, Kunnen SJ, Gansevoort RT, Breuning MH, de Heer E, Peters DJ: Curcumin inhibits cystogenesis by simultaneous interference of multiple signaling pathways: In vivo evidence from a Pkd1-deletion model. *Am J Physiol Renal Physiol* 300: F1193–F1202, 2011
39. Takakura A, Nelson EA, Haque N, Humphreys BD, Zandi-Nejad K, Frank DA, Zhou J: Pyrimethamine inhibits adult polycystic kidney disease by modulating STAT signaling pathways. *Hum Mol Genet* 20: 4143–4154, 2011
40. Zhang L, Badgwell DB, Bevers JJ 3rd, Schlessinger K, Murray PJ, Levy DE, Watowich SS: IL-6 signaling via the STAT3/SOCS3 pathway: Functional analysis of the conserved STAT3 N-domain. *Mol Cell Biochem* 288: 179–189, 2006
41. Talbot JJ, Shillingford JM, Vasanth S, Doerr N, Mukherjee S, Kinter MT, Watnick T, Weimbs T: Polycystin-1 regulates STAT activity by a dual mechanism. *Proc Natl Acad Sci U S A* 108: 7985–7990, 2011
42. Fleck C: Determination of the glomerular filtration rate (GFR): Methodological problems, age-dependence, consequences of various surgical interventions, and the influence of different drugs and toxic substances. *Physiol Res* 48: 267–279, 1999
43. Johnson HA, Vera Roman JM: Compensatory renal enlargement. Hypertrophy versus hyperplasia. *Am J Pathol* 49: 1–13, 1966
44. Kierulf-Lassen C, Nielsen PM, Qi H, Damgaard M, Laustsen C, Pedersen M, Krag S, Birn H, Nørregaard R, Jespersen B: Unilateral nephrectomy diminishes ischemic acute kidney injury through enhanced perfusion and reduced pro-inflammatory and pro-fibrotic responses. *PLoS One* 12: e0190009, 2017
45. Stamatiades EG, Tremblay ME, Bohm M, Crozet L, Bisht K, Kao D, Coelho C, Fan X, Yewdell WT, Davidson A, Heeger PS, Diebold S, Nimmerjahn F, Geissmann F: Immune monitoring of trans-endothelial transport by kidney-resident macrophages. *Cell* 166: 991–1003, 2016
46. Zimmerman KA, Bentley MR, Lever JM, Li Z, Crossman DK, Song CJ, Liu S, Crowley MR, George JF, Mrug M, Yoder BK: Single-cell RNA sequencing identifies candidate renal resident macrophage gene expression signatures across species. *J Am Soc Nephrol* 30: 767–781, 2019

Received: December 13, 2019 **Accepted:** February 14, 2020